

# Kinetics of Humic Acid Adsorption at Solid-Water Interfaces

MARCELO J. AVENA<sup>†</sup> AND  
LUUK K. KOOPAL\*

Laboratory for Physical Chemistry & Colloid Science,  
Wageningen Agricultural University, P.O. Box 8038,  
6700 EK Wageningen, The Netherlands

The adsorption kinetics of purified Aldrich humic acid (PAHA) onto hydrophilic ( $\text{Fe}_2\text{O}_3$  and  $\text{Al}_2\text{O}_3$ ) and hydrophobic (polystyrene and silanized  $\text{SiO}_2$ ) surfaces are studied by reflectometry. The initial rate of adsorption depends on the rate of transport and the rate of attachment. Attachment on hydrophilic surfaces is relatively fast at low pH where surface and HA attract each other electrostatically. Moreover, carboxylic and phenolic groups are exposed to the outside of the HA molecules, and these groups form complexes with surface hydroxyl groups. Due to the high attachment rate the process is transport-limited. At high pH, where surface and HA repel each other electrostatically, attachment is slow, and the adsorption rate is attachment-limited. At hydrophobic surfaces attachment of HA takes place through hydrophobic attraction. Hydrophobic groups are hidden in the inner part of HA molecules, and structural rearrangements are required before attachment can occur. The slow attachment leads to an attachment-limited rate. Increasing the pH increases the number of charged groups at the outside of the molecules, and the rate of attachment becomes even slower. Adsorption rate variations with electrolyte concentration also reveal the dynamics and flexibility of the HA molecules and the sensitivity of attachment for electrostatic effects.

## Introduction

Humic substances such as humic acids (HA) and fulvic acids (FA) are natural weak polyelectrolytes that are very active in binding ions and organic molecules (1, 2). These properties make HA and FA important in regulating the speciation, mobility, and transport of ions, nutrients, and contaminants in soils and aquifers (3, 4). Humic substances have also a relatively strong affinity for oxide surfaces and tend to be attached to particulate matter (5–8). Thus, the reactive properties of HA and FA can be significantly modified by the presence of oxide or clay particles and vice versa. Therefore, the mechanisms of binding of humics to solid surfaces have to be known in order to improve the understanding of the role that these substances play in the environment.

The adsorption of HA and FA on oxide or clay surfaces has been experimentally studied as a function of different variables such as pH, electrolyte concentration, type of humic, etc. (7–12). Most of the studies were performed by “equilibrium” adsorption experiments in which a mixture of

adsorbate and adsorbent is “equilibrated” at the desired conditions, and the adsorbed amount or the remaining nonadsorbed amount is then measured. This kind of experiments allows studying the effects of the different variables on the affinity of the humics for different surfaces. Together with adsorption experiments, desorption studies can be performed in order to test the reversibility of the process and to gain insights on the HA-solid surface interaction. Although very interesting aspects of this interaction have been revealed by desorption studies, only a few articles have been published so far (5, 13), and much work has still to be done in this field.

Detailed studies about the kinetics of the adsorption or desorption processes have not appeared in the literature yet. Most of the reports point out that the adsorption is fast but do not present a detailed kinetic analysis of the process (6, 11). Due to the fact that the initial steps of adsorption take place quickly, there are not many techniques that are able to follow the attachment of molecules in a short time scale. This scarcity of techniques may be the main reason kinetics has received little attention. Pinheiro et al. (14) successfully applied alternating current voltammetry to study the adsorption of HA on the Hg/aqueous solution interface. They have shown that the kinetics is affected not only by transport processes but also by reactions at the surface as well as by electrostatic interactions between adsorbing molecules and previously adsorbed ones. Unfortunately, voltammetry cannot be easily applied to study the mentioned processes on metal oxides or clays. Recently, Avena and Koopal (13) showed that reflectometry can be used to follow the kinetics of HA adsorption and desorption on an iron oxide surface. It was shown that the rate of adsorption levels off strongly after the first 100 s. In 0.1 M salt concentration and for a HA concentration of 50 mg/L, about 1.5 mg/m<sup>2</sup> of material is adsorbed in the first 100 s at pH 3.25. Much slower processes that can continue for many hours (8) follow this quick process. The slow adsorption processes can be attributed to the presence of long-range electrostatic repulsion and/or rearrangements in the adsorbed layer either by conformation changes or by exchange of adsorbed HA molecules with newly arriving ones of larger molecular mass. Polydispersity effects on the adsorption have been studied both experimentally (by replacement of preadsorbed FA by HA) and theoretically by Vermeer and Koopal (8).

The aim of this article is to analyze the fast initial adsorption step in more detail by investigating the influence of supporting electrolyte concentration, pH and HA concentration on the adsorption kinetics of a HA sample on various surfaces. The processes are followed by reflectometry in a stagnation point flow cell, and the results are analyzed on the basis of a simple model for the adsorption kinetics. The slow processes following the initial adsorption step will not be considered.

## Materials and Methods

Chemicals were p.a. quality, and high purity water was used. All experiments were performed at 25 °C at a supporting  $\text{KNO}_3$  concentration ranging between 0.003 and 0.8 M and in the pH range 3.5–10.0.

**Humic Acid.** A purified Aldrich humic acid (PAHA) was used. The method of purification of this sample and some physical and chemical properties have been reported previously (7, 15, 16). The elemental analysis of PAHA is (wt) C, 55.8%; O, 38.9%; H, 4.6%; and N, 0.6%, and its total acidity is about 5 mmol/g. According to Vermeer (15) the weight average molecular mass,  $M_w$ , of PAHA obtained by size exclusion chromatography using proteins as standards equals

\* Corresponding author phone: +31 317 482629; fax: +31 317 483777; e-mail: koop@fenk.wau.nl.

<sup>†</sup> On leave of absence from INFIQC, Departamento de Físico-química, Facultad de Ciencias Químicas, Universidad Nacional de Córdoba, Córdoba, Argentina.

20 kD. Static light scattering measurements showed molecular masses of 15–40 kD for the fractions collected around the peak of the distribution function and indicated that the polydispersity of PAHA is only moderate. In view of these results the value  $M_w = 20$  kD is adopted for PAHA. Beckett and Hart (17) have obtained for Aldrich humic acid a somewhat lower value of  $M_w = 14.5$  kD with field flow fractionation. By viscometry it was shown that the molecules of the PAHA behave as flexible entities that can swell or shrink somewhat in response to changes in pH and ionic strength (16). An increase in the ionic strength or a decrease in the pH lead to molecular shrinkage. The effect of pH in changing the hydrodynamic volume of the molecules is significant at low electrolyte concentration (i.e., 0.001 M) but is almost negligible at 0.1 M or higher electrolyte concentrations.

Stock solutions of HA (2–3 g/L) were prepared by dissolving overnight freeze-dried HA in a KOH solution at pH between 10 and 11. This ensures complete dissolution of the sample. The working solutions (usually 30 or 50 mg/L) were made by diluting the stock solution with the supporting electrolyte, KNO<sub>3</sub>.

**Surfaces.** Four surfaces with different degrees of hydrophobicity were investigated: Fe<sub>2</sub>O<sub>3</sub>, Al<sub>2</sub>O<sub>3</sub>, silanized SiO<sub>2</sub> (SiO<sub>2</sub>-sil), and polystyrene (PS). Strips of silicon wafers with a SiO<sub>2</sub> surface layer were used as the starting materials, and they were treated in different ways in order to obtain wafers bearing the desired surfaces. The wafers were of the Czochralsky type and were obtained from Aurel GmbH (Germany). The SiO<sub>2</sub> surface layer was grown by oxidation of the silicon wafer in air at around 1000 °C for 1 h.

The iron oxide and aluminum oxide layers were deposited over the silica layer by reactive sputtering of Fe and Al, respectively, in an oxygen atmosphere. This was carried out at Phillips Laboratories at Eindhoven, The Netherlands. Electron microscopy and atomic force microscopy revealed that the surfaces of iron oxide and aluminum oxides layers were very smooth and flat, with no cracks or irregularities. These surfaces were highly hydrophilic, with a contact angle of water lower than 5°. The isoelectric point (iep) of the surfaces was roughly estimated by adsorption of positively and negatively charged strong polyelectrolytes using reflectometry. They resulted to be around 4.5 for Fe<sub>2</sub>O<sub>3</sub> and around 6.5 for Al<sub>2</sub>O<sub>3</sub>. These iep values are lower than the respective iep or points of zero charge of pure crystalline iron and aluminum oxides (18). This behavior has also been reported for titanium and iridium coatings on silica (19, 20). It might be due to a surface that is less well structured than that of ordinary crystalline oxides (19), or it may be an indication of the presence of adsorbed anionic impurities.

The silanized silica surface (SiO<sub>2</sub>-sil) was prepared by dip-coating the oxidized wafer strips in a 1.6% solution of dichlorodimethylsilane in 1,1,1-trichloroethane for 30 min. The strip surface resulted to be hydrophobic, with a contact angle of around 90°. The silanization decreases the number of ionizable OH groups at the surface, and the remaining OH groups are embedded in a layer with a low dielectric constant. As a result it is to be expected that even at high pH values such a surface will hardly be charged.

The PS surface was prepared by first immersing the Si/SiO<sub>2</sub> wafer strips for 30 min in a 100 ppm solution of a Poly4VinylPyridine-PolyStyrene copolymer (Polymer Source Inc., Laval, Canada) in chloroform. The vinylpyridine groups anchor onto the silica surface, and the polystyrene chains protrude from it. Subsequently, a 4 g/L polystyrene ( $M = 443\,200$ ) solution in toluene was spin coated (2000 rpm) on the pretreated wafer. The wafers were then placed in an oven at 100 °C (glass temperature of PS) overnight. The thickness of the so-prepared PS layers is about 20 nm, and the PS surface has a contact angle of about 90°. The deposited PS layer is uncharged.

TABLE 1. List of the Different Wafers Used and Their Characteristics<sup>a</sup>

surface	Fe <sub>2</sub> O <sub>3</sub>	Al <sub>2</sub> O <sub>3</sub>	SiO <sub>2</sub> -sil	PS
support	Si	Si	Si	Si
	$n = 3.85$	$n = 3.85$	$n = 3.85$	$n = 3.85$
inner layer	SiO <sub>2</sub>		SiO <sub>2</sub>	SiO <sub>2</sub>
	$n = 1.46$		$n = 1.46$	$n = 1.46$
	$d = 80$ nm		$d = 80$ nm	$d = 80$ nm
outer layer	Fe <sub>2</sub> O <sub>3</sub>	Al <sub>2</sub> O <sub>3</sub>	monolayer of SiOC(CH <sub>3</sub> ) <sub>3</sub>	layer of (PVP)-PS
	$n = 2.96$	$n = 1.63$		$n = 1.59$
	$d = 55$ nm	$d = 86$ nm		$d = 20$ nm
1/A <sub>s</sub> (mg/m <sup>2</sup> )	−22	32	17	22
contact angle	0°–5°	0°–5°	85°–90°	85°–90°

<sup>a</sup> The values  $dn/dc_{HA} = 0.28$  cm<sup>3</sup>/g,  $n_{HA} = 1.363$ ,  $d_{HA} = 5$  nm,  $n_{water} = 1.333$ ,  $\theta_i = 70.6^\circ$ , and  $\lambda = 632.8$  nm were also used in calculations.

**Reflectometry.** Adsorption measurements were performed by reflectometry in a stagnation-point flow cell as described before (13). For details of the method we refer to Dijt et al. (21). Upon adsorption of the HA to the surface the signal  $S$  of the reflectometer changes by an amount  $\Delta S$ . In adequate conditions (22), the relative change of the signal,  $\Delta S/S_0$ , is proportional to the adsorbed amount  $\Gamma$

$$\Gamma = \frac{1}{A_s} \frac{\Delta S}{S_0} \quad (1)$$

where  $A_s$  is the sensitivity factor and  $S_0$  the signal of the bare surface.  $A_s$  depends not only on the thickness  $d$  and the refractive indexes  $n$  of silicon, the surface layers and the solution, but also on the refractive index increment  $dn/dc$  of the adsorbed HA layer, the angle of incidence  $\theta_i$ , and the wavelength  $\lambda$  of the laser beam. The characteristics of the materials that have been used to calculate  $A_s$  (23) and the values of  $A_s$  for different surfaces are listed in Table 1.

A typical adsorption experiment consisted in equilibrating the wafer by flowing a supporting electrolyte solution of the desired pH. Once a stable baseline was obtained, the flux was switched to a HA solution of the same pH and electrolyte concentration, and the change in the signal was followed as a function of time for a few minutes.  $\Delta S$  was converted to  $\Gamma$  using eq 1 and the  $A_s$  values shown in Table 1.

## Theory

In the initial steps of the adsorption of HA on a solid surface two processes are important: (1) transport from the bulk solution to the subsurface plane adjacent to the surface and (2) attachment to the surface. These two processes will be considered in more detail. Rearrangements in the adsorbed layer due to reconformations and polydispersity effects and/or other slow adsorption processes that may become evident at relatively long times can be neglected in the initial stages of the adsorption process.

**Transport.** In a steady-state situation, the flux  $J$  of adsorbing molecules in a stagnation point flow is described by the following equation (21)

$$J = KD^{2/3}(c_b - c_s) \quad (2)$$

where  $D$  is the diffusion coefficient of the adsorbing HA molecules,  $c_s$  and  $c_b$  are their concentration in the subsurface plane adjacent to the surface and in the bulk solution, respectively, and  $K$  is a constant for dilute solutions. The magnitude of  $K$  is given by the hydrodynamics of the cell used in the experiments and the flow rate of solution (13, 21). For a given cell and a known flow rate  $K$  can be calibrated using a polymer with a known diffusion coefficient.

For spherical molecules,  $D$  is related to the hydrodynamic radius of the molecules,  $r$ , through the Stokes–Einstein

equation

$$D = \frac{kT}{6\pi\eta r} \quad (3)$$

where  $k$  is the Boltzmann constant,  $T$  is the temperature, and  $\eta$  is the viscosity of the aqueous solution. For HA molecules that need not to be spherical eq 3 is an approximation; moreover the pH and ionic strength will influence  $D$ . An increase in the electrolyte concentration and a decrease in pH will increase  $D$  because the hydrodynamic volume of the HA molecules decreases (16). If aggregation of the molecules takes place,  $D$  will decrease significantly.

To write eq 2 in a slightly different way, the flux for  $c_s = 0$  can be introduced

$$J_0 = KD^{2/3}c_b \quad (4)$$

and eq 2 thus becomes

$$J = J_0 \frac{(c_b - c_s)}{c_b} \quad (5)$$

Above it has been assumed that the adsorbing molecules are monodisperse. In the case of a polydisperse sample the initial rate of adsorption is mainly determined by the lower molecular mass fraction, because these molecules have the highest diffusion coefficients. However, it should be realized that the solution concentration of these molecules is only a fraction of  $c_b$ . Therefore, the calculation of the diffusion coefficient from the observed adsorption rates, the known value of  $K$  and the total concentration  $c_b$ , leads to an apparent diffusion coefficient that is lower than the true  $D$  value of the adsorbing fraction. The calculated value is probably a reasonable estimation of the average diffusion coefficient of the sample.

**Attachment.** A simple attachment/detachment model considers that (1) a molecule adsorbs with rate coefficients  $k_a$  and  $k_d$  for adsorption and desorption respectively, (2) the adsorption occurs on the fraction of the surface that is bare, and (3) the desorption is a function of the adsorbed amount. The net rate of adsorption or the net flux of molecules from the subsurface layer to the surface is then given by

$$d\Gamma/dt = k_a c_s \phi - k_d f(\Gamma) \quad (6)$$

where  $\phi$  is the available surface area for adsorption and  $f(\Gamma)$  is related to the area occupied by the adsorbate molecules. Hence, in general both  $\phi$  and  $f(\Gamma)$  are a function of the adsorbed amount and the structure of the adsorbed layer. In addition, the presence of other molecules or ions that compete for the surface sites with the adsorbate molecules will affect  $\phi$ .

The parameters  $k_a$  and  $k_d$  can be written in the form of the Arrhenius equation; they are related to the activation energy for adsorption and desorption, respectively, and a frequency factor that can include orientation or steric effects (24). The activation energies depend on the state of hydration of the surface and the adsorbate molecules, on the interactions between the surface and the adsorbate, on the adsorbate-adsorbate interactions, and on the conformation of the molecules in the adsorbed layer.

As only the *initial* adsorption rate,  $(d\Gamma/dt)_i$ , will be considered, eq 6 can be simplified even further. Under this condition the amount of adsorbed molecules is nearly zero, rearrangements and lateral interactions in the adsorbed layer can be neglected, and eq 6 reduces to

$$(d\Gamma/dt)_i = k_a c_s \phi \quad (7)$$

The value of  $k_a$  will now only depend on surface-adsorbate interactions, and  $\phi$  is now determined by the presence of competing inorganic salt ions only. If no competition with salt ions takes place  $\phi = 1$  and in case of competition  $\phi < 1$ .

**Transport and Attachment.** Continuity in the subsurface layer means that the flux of molecules from the bulk to the subsurface layer just equals the net flux of molecules from the subsurface layer to the surface, i.e.,  $J = d\Gamma/dt$ . This leads to the following expression for the *initial* adsorption rate

$$(d\Gamma/dt)_i = \frac{k_a \phi J_0 c_b}{k_a \phi c_b + J_0} \quad (8a)$$

which can also be written as

$$(d\Gamma/dt)_i = \frac{k_a \phi K D^{2/3} c_b}{k_a \phi + K D^{2/3}} \quad (8b)$$

From this general equation for the initial adsorption rate two important limiting cases can be deduced:

(a) If  $k_a \phi \gg J_0$  the rate of attachment is much faster than the rate of transport, and the process becomes *transport-limited*

$$(d\Gamma/dt)_i = J_0 = K D^{2/3} c_b \quad (k_a \phi \gg J_0) \quad (9)$$

from which the diffusion coefficient can be determined when  $K$  is known.

(b) If  $k_a \phi \ll J_0$  the rate of attachment is much lower than the rate of transport, and the process becomes *attachment-limited*

$$(d\Gamma/dt)_i = k_a \phi c_b \quad (k_a \phi \ll J_0) \quad (10)$$

from which the product  $k_a \phi$  can be obtained.

## Results and Discussion

**Calibration.** To be able to estimate the diffusion coefficient of the adsorbing HA molecules, it is necessary to calibrate the value of  $K$ . Calibration was performed by measuring the initial adsorption rate of a nearly monodisperse poly(ethylene oxide) sample (Polymer Laboratories,  $M_w/M_n = 1.09$ ,  $M = 246\,000$  and  $D = 1.55 \times 10^{-11} \text{ m}^2 \text{ s}^{-1}$  (25)) on a silica surface under transport-limited conditions (21). At  $c_b = 13.8 \text{ mg/L}$  and a solution flow of  $1.3 \text{ mL/s}$ , the initial adsorption rate was  $0.025 \text{ mg s}^{-1} \text{ m}^{-2}$ . According to eq 9 this results in  $K = 30 \text{ s}^{-1/3} \text{ m}^{-1/3}$ .

**Effect of the Humic Acid Concentration.** To investigate the effect of the PAHA concentration on the adsorption rate a series of freshly prepared PAHA solutions ( $6\text{--}50 \text{ mg/L}$ ) of  $\text{pH } 3.9 \pm 0.1$  and an electrolyte concentration of  $0.1 \text{ M}$  were used. Figure 1 shows a typical result for PAHA adsorption on iron oxide. Initially only the supporting electrolyte was flowing, and the baseline is observed. Then the flow was switched to the HA solution, and a fast change in the signal due to adsorption is noted. Figure 1 indicates that the initial adsorption is relatively fast even for low concentrations. However, already after  $20\text{--}80 \text{ s}$  the adsorption rate becomes very slow. As pointed out before (8, 13), this slow process may last for hours and is related to long-range electrostatic repulsion between incoming molecules and the adsorbed layer, rearrangements in the adsorbed layer by conformational changes, and/or by exchange of adsorbed relatively small HA molecules by large HA molecules. These long time effects will be considered in a future publication. Although Figure 1 applies to adsorption on  $\text{Fe}_2\text{O}_3$ , qualitatively similar curves are found for the other surfaces and at different pH values and/or salt concentrations.



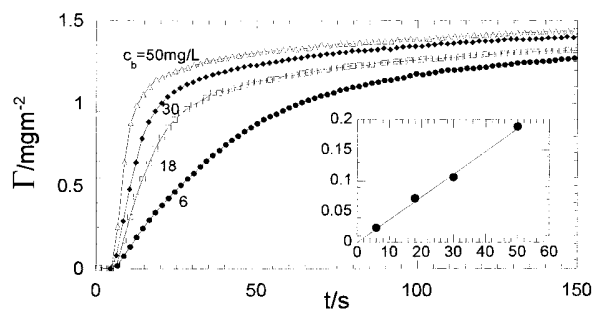


FIGURE 1. Effect of the HA concentration on the adsorption behavior of PAHA on  $\text{Fe}_2\text{O}_3$ . Flow rate: 0.625 mL/min;  $c_{\text{KNO}_3} = 0.1 \text{ M}$ ;  $\text{pH} = 3.9 \pm 0.1$ . The HA concentration,  $c_{\text{PAHA}} = c_b$ , is indicated in the figure. The inset shows the variation of the initial adsorption rate,  $(d\Gamma/dt)_i$ , in  $\text{mg m}^{-2} \text{ s}^{-1}$ , as a function of  $c_b$  in  $\text{mg/L}$ .

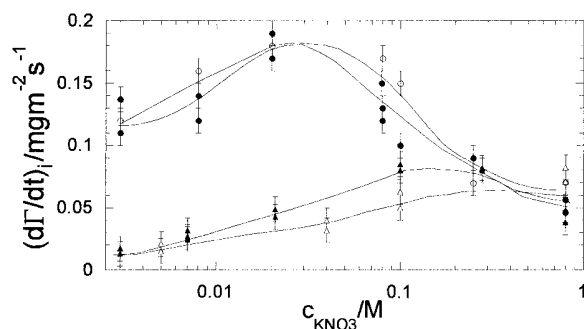


FIGURE 2. Effect of the electrolyte concentration on the initial adsorption rate of PAHA on the different surfaces studied: (●)  $\text{Fe}_2\text{O}_3$ ; (○)  $\text{Al}_2\text{O}_3$ ; (▲)  $\text{SiO}_2\text{-sil}$ ; and (△) PS. Flow rate: 1.3 mL/min;  $\text{pH} = 3.9 \pm 0.1$ ,  $c_{\text{PAHA}} = 30 \text{ mg/L}$ .

At high HA concentrations the adsorption is so fast that only a few data points can be used to estimate the initial adsorption rate. On the other hand, at low HA concentrations where the  $\Gamma$  vs time curve has more data points, the calculated initial adsorption rate may be affected by some drift of the baseline. Due to these uncertainties, the relative error in the determination of  $(d\Gamma/dt)_i$  is around  $\pm 10\%$  (obtained from repeated experiments).

Figure 1 shows that  $(d\Gamma/dt)_i$  increases by increasing the HA concentration, in agreement with eq 8b. The linear dependence of the initial adsorption rate with  $c_b$  can be seen in the inset of the figure. A deviation from a straight line toward lower adsorption rates can be sometimes observed for HA concentrations higher than 50  $\text{mg/L}$ . This behavior is more evident for aged solutions of low pH ( $\text{pH} < 3.5$ ) and high electrolyte concentration. It is due to aggregation of HA molecules which results in a lower concentration of relatively small HA molecules that quickly diffuse and/or in a decrease of the average diffusion coefficient.

**Effect of the Salt Concentration.** The effects of the salt concentration on the initial adsorption rate at  $\text{pH } 3.9 \pm 0.1$  for the four surfaces studied are shown in Figure 2. The results for  $\text{Al}_2\text{O}_3$  are similar to those for  $\text{Fe}_2\text{O}_3$ , and the results for PS are comparable to those for  $\text{SiO}_2\text{-sil}$ . In all cases  $(d\Gamma/dt)_i$  depends on the electrolyte concentration. For the hydrophilic surfaces a clear maximum is observed. This maximum is much weaker or absent for the hydrophobic surfaces. The position of the maximum is around 0.03 M for Al and Fe oxides and around 0.2 M for the hydrophobic silica surface.

In the case of the hydrophilic  $\text{Fe}_2\text{O}_3$  and  $\text{Al}_2\text{O}_3$  surfaces an electrostatic attraction between the surfaces and the molecules has to be considered because surface and HA are oppositely charged at  $\text{pH } 3.9$ . Due to the long-range nature of the coulomb attraction, the activation energy for attachment will be affected. An increase in the salt concentration

will decrease the electrostatic attraction and, hence, increase the activation energy for attachment. Therefore, when attachment is the limiting process, a decrease in  $(d\Gamma/dt)_i$  by increasing the electrolyte concentration is expected. Figure 2 shows the opposite trend at  $\text{pH } 3.9$ . This indicates that the activation energy for attachment is rather low and that the process is transport-limited. Under transport limitation and in the absence of aggregation, variations in the rate are expected to be only dependent on  $D$  (see eq 9). The increase in the adsorption rate by increasing the electrolyte concentration from 0.003 to 0.03 M should then correspond with an increase in the diffusion coefficient of the adsorbing molecules. Calculations based on eq 9 and the calibrated value of  $K$  lead to apparent diffusion coefficients of  $6 \times 10^{-11}$  and  $9 \times 10^{-11} \text{ m}^2 \text{ s}^{-1}$  for HA molecules at 0.003 and 0.03 M electrolyte, respectively. These values are in good agreement with those reported by Cornell et al. (26), who measured mass transfer coefficients for a purified Aldrich humic sample. The diffusion coefficients result in respective hydrodynamic radii of 3.6 and 2.4 nm indicating molecular shrinkage by increasing the electrolyte concentration. These results are in qualitative agreement with previously reported intrinsic viscosities of PAHA (16) that indicate a decrease in the average hydrodynamic radius by about 10% when at  $\text{pH} = 4$  the salt concentration is increased from  $10^{-3}$  to  $10^{-2} \text{ M}$ . At higher pH values this difference increases. The above observations support the conclusion that up to 0.03 M  $\text{KNO}_3$  the adsorption process of HA to iron and aluminum oxides is transport-limited. The increase in the adsorption rate with increasing salt concentration is due to a decrease of the molecular radius of the adsorbing molecules, which corresponds with an increase of the diffusion coefficient.

When the electrolyte concentration becomes higher than 0.03 M, the initial adsorption rate on the hydrophilic surfaces decreases. The adsorption rate at 0.03 M is around three times higher than the rate at 0.8 M. Under transport-limited conditions an increase in the rate with increasing ionic strength would be expected, due to an increase in  $D$ ; however, this trend can be reversed if aggregation of molecules takes place. When the process is transport-limited, the ratio of the initial adsorption rates at conditions A and B and under transport limitation equals (eqs 9 and 3)

$$\frac{(d\Gamma/dt)_{i,A}}{(d\Gamma/dt)_{i,B}} = \left(\frac{r_B}{r_A}\right)^{2/3} \frac{c_{b,A}}{c_{b,B}} \quad (11)$$

where  $r_A$  and  $r_B$  represent the hydrodynamic radii of the molecules at the conditions A and B, respectively, and  $c_{b,X}$  ( $X = A, B$ ) is the concentration of the adsorbing species. Equation 11 indicates that for  $c_{b,A} = c_{b,B}$  a 3-fold decrease in the rate should correspond with a 5-fold increase in the hydrodynamic radius. It is also possible to assume that the fraction of small molecules that diffuses most quickly is still available but that the concentration of this fraction is diminished. In this case a 3-fold concentration decrease is required to explain the results. For  $\text{KNO}_3$  concentrations up to about 0.1 M both mechanisms are unlikely, because aggregation of the HA molecules is weak or absent. HA molecules can form large aggregates, but this will occur at salt concentrations higher than 0.1 M (27–30). Aggregation of PAHA can be observed by visual inspection of the solutions at  $\text{pH} = 3.9$  for electrolyte concentrations ranging 0.3 to 0.8 M, if the solutions are at rest for some time. Only for these high salt concentrations aggregation will contribute significantly to the decrease in the rate of adsorption.

In the electrolyte concentration range of 0.03–0.1 M  $\text{KNO}_3$  it is most likely that the attachment process affects the overall adsorption rate. This will be the case when the transport and attachment rates become comparable. At  $\text{pH} = 3.9$ , where the surface and the HA are oppositely charged, an increase

in the electrolyte concentration will increase the activation energy for attachment due to screening of the electrostatic attraction. Moreover, competition with electrolyte ions for the adsorption sites may become important. Screening of the surface-adsorbate attraction has been observed for both low (31, 32) and high molecular mass (33) charged organics. Competition effects on the rate of adsorption have been advocated by Hoogeveen et al. (20). These authors observed a sharp decrease of the initial adsorption rate to nearly zero for the adsorption of quaternized polyvinyl pyridine (PVP<sup>+</sup>) on a negatively charged TiO<sub>2</sub> surface at ionic strength values between 0.02 and 0.3 M, depending on the PVP<sup>+</sup> molecular mass. In the case of PAHA adsorption on Al and Fe oxide surfaces both screening and competition are likely to contribute to the observed decrease in the attachment rate when the salt concentration is increased.

According to Figure 2 the initial adsorption rates on the hydrophobic SiO<sub>2</sub>-sil and PS surfaces are also similar. At low electrolyte concentrations the rates are much lower than those on the hydrophilic surfaces are. As the transport rate of the HA molecules to the hydrophobic and the hydrophilic surfaces is the same, this indicates that the adsorption on SiO<sub>2</sub>-sil and PS is attachment limited. Since competition with electrolyte is unlikely on hydrophobic surfaces and low electrolyte concentrations, the difference between the adsorption rate on the Fe and Al oxides and the adsorption rate on the SiO<sub>2</sub>-sil and PS surfaces must be due to changes in  $k_a$ . This can be accomplished by changes in either the activation energy for adsorption or the frequency factor. As both surfaces are uncharged (pH = 3.9), the presence of a repulsive electrostatic barrier cannot be used to explain the behavior. Therefore, the low initial adsorption rates on SiO<sub>2</sub>-sil and PS have to be a consequence of the surface hydrophobicity. Apparently, the hydrophobicity leads to a low  $k_a$  value, i.e., large activation energy for attachment. In aqueous solutions most of the hydrophobic parts of the HA molecules are screened from contacts with water molecules by the hydrophilic groups, that is to say, the hydrophobic parts tend to be in the inner part of the molecule where the water content is relatively low. Therefore, upon arrival at the surface the HA molecules expose mainly hydrophilic groups toward the surface. Hydrophobic attachment can only take place after some structural rearrangements of the HA molecules. This results in a relatively low  $k_a$  value and an attachment-limited process.

Increasing the salt concentration up to about 0.1 M leads to an increase in the initial adsorption rate for both hydrophobic surfaces. This may be due to the fact that the size of the HA molecules decreases with increasing salt concentration. Consequently the probability of finding hydrophobic groups near the periphery of the HA molecules becomes higher and  $k_a$  increases. By introducing in eq 8 the values of  $K$  and  $D$  as calculated before (no aggregation) and assuming that  $\phi = 1$ , a value of  $k_a = 0.8 \times 10^{-6} \text{ m s}^{-1}$  is found at 0.003 M salt and  $k_a = 2.6 \times 10^{-6} \text{ m s}^{-1}$  at 0.03 M. This shows that  $k_a$  increases substantially by increasing the electrolyte concentration. The fact that at pH = 3.9 the rates on the two hydrophobic surfaces increase up to 0.1 M salt is a further indication that HA aggregation is indeed negligible under these conditions.

The slight decrease or leveling off of the adsorption rate at electrolyte concentrations between 0.2 and 0.8 M is most probably due to molecular aggregation. A rather convincing indication that the adsorption rate at these very high electrolyte concentrations becomes transport limited is the fact that the rate is hardly dependent on the nature of the substrate. Due to molecular aggregation the adsorption rate is transport-limited, without depending on the type and properties of the adsorbing surface.

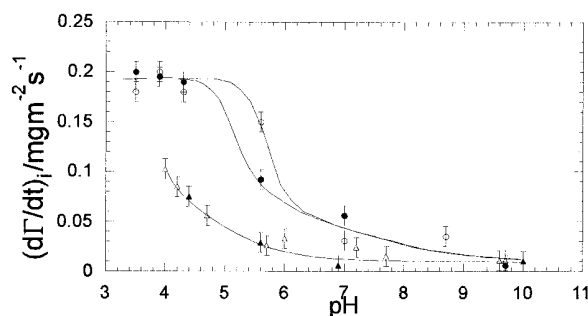


FIGURE 3. Effect of the solution pH on the initial adsorption rate of PAHA on the different surfaces studied: (●) Fe<sub>2</sub>O<sub>3</sub>; (○) Al<sub>2</sub>O<sub>3</sub>; (▲) SiO<sub>2</sub>-sil; and (△) PS. Flow rate: 1.3 mL/min;  $C_{\text{KNO}_3} = 0.1 \text{ M}$ ,  $C_{\text{PAHA}} = 50 \text{ mg/L}$ .

**Effect of the pH.** Figure 3 shows the effects of the solution pH on initial adsorption kinetics on the four surfaces studied. The initial adsorption rate on Fe<sub>2</sub>O<sub>3</sub> and Al<sub>2</sub>O<sub>3</sub> is high at low pH values and remains constant until pH around 5. Up to this pH the rate of transport dominates. In more alkaline solutions, the rate is pH dependent and decreases as the pH increases. This decrease cannot be explained by assuming variations in  $D$  due to swelling of the molecules upon an increase in pH. The initial adsorption rate at pH = 4 is around 10 times higher than the rate at pH = 10, and according to eq 11 this corresponds to about a 30-fold increase in the hydrodynamic radius, which means about a 30 000-fold increase in the hydrodynamic volume. Such an increase in volume is definitely not the case for PAHA because it is known that its molecular volume remains almost invariable with pH at 0.1 M electrolyte (16). Moreover, the maximum variation in the volume with a variation in pH as measured for a series of HA samples at 0.001 M electrolyte concentration was only a factor of 3 (16), which is still 4 orders of magnitude lower than the value calculated above. Aggregation of particles cannot be postulated to explain the decrease in the adsorption rate either. An increase in the negative charge and potential of the HA molecules upon an increase in the pH will counteract aggregation (27). The relatively large decrease in the adsorption rate by increasing the pH has to be a consequence of a decrease in  $k_a\phi$ .

The shape of the rate vs pH curves suggests that the main factor that affects the adsorption rate is of electrostatic origin. At pH <  $\text{iep}$  the attachment is promoted by the electrostatics, and the adsorption process is transport-limited. At pH >  $\text{iep}$  the situation is reversed, negative charges of the molecules and the surfaces generate a strong electrostatic barrier for adsorption and the process becomes attachment limited. Increasing the pH decreases  $k_a$  significantly, and this results in a steep decrease of the rate. The slow rate of attachment that occurs when polyelectrolyte and surface repel each other electrostatically is a very important phenomenon with polyelectrolyte adsorption. It makes polyelectrolyte adsorption kinetics distinctly different from polymer adsorption kinetics.

The initial adsorption rate of PAHA on hydrophobic SiO<sub>2</sub>-sil and PS also decreases by increasing the pH, but the decrease starts already at low pH and is very similar for both surfaces. Although it is possible that the SiO<sub>2</sub>-sil surface carries some charges at high pH values, the similarity of the behavior on the two surfaces strongly suggests that electrostatics is not playing a major role. This corresponds with the expectation that the remaining OH groups on the SiO<sub>2</sub>-sil surface are very difficult to deprotonate.

Again the hydrophobicity of the surfaces is the most important factor. As the pH increases the charge of the HA molecules increases, and more and more charged groups occur at the periphery of the molecules. This decreases the

possibility of attachment to the surface by the hydrophobic groups. A significant decrease in the rate is observed up to pH = 7. Beyond this pH the attachment rate is very slow, and further charging of the HA molecules has no effect. The fact that the rate becomes similar to that at the hydrophilic surfaces at high pH is probably a coincidence that is related to the fact that the rate is very slow anyhow.

Summarizing, the initial adsorption kinetics of humic acids on solid surfaces is a rather complex process that depends on the nature of the surface and the solution conditions. The attachment is fast on hydrophilic surfaces if electrostatic repulsion is absent. Since HA has a high number of carboxylic and phenolic groups exposed to the outside of the molecules, the attachment with the surface hydroxyl groups of Fe and Al oxide surfaces is a quick process. The overall rate of adsorption is transport-limited. Upon increasing the pH the particles and the surface become both negative, an electrostatic barrier slows down the attachment process, and the adsorption becomes attachment-limited. An increase in the salt concentration decreases the electrostatic interactions, and this affects both the rate of attachment and the rate of transport. For pH <  $p_{\text{iep}}$  the rate of attachment will decrease, whereas for pH >  $p_{\text{iep}}$  this rate increases. The rate of transport will always increase upon an increase of the salt concentration, unless the salt concentration becomes so high that aggregation takes place.

At hydrophobic surfaces where attachment takes place through hydrophobic attractions, the attachment is relatively slow because most of the hydrophobic groups of the HA are not at the periphery of the molecule, and structural changes have to take place before the adsorption can occur. Expansion of the HA molecules due to an increase in pH or a decrease in the salt concentration slows the rate further down because the hydrophobic groups are better screened by the charged groups at the outside of the molecules.

At salt concentrations larger than 0.2 M aggregation of the HA molecules is important, and in the absence of electrostatic repulsion between surface and adsorbate the adsorption becomes diffusion-limited independently of the type of surface. When surface and HA have the same charge sign, attachment limitation may even at these high salt concentrations be a relevant factor.

Although most of the surfaces in soils and aquifers belong to oxide-like materials with high hydrophilicity, our study of the adsorption process at a series of surfaces has revealed interesting properties of the HA molecules. Variations in the initial adsorption rate with both the electrolyte concentration and the pH reveal the dynamics and flexibility of HA molecules. Variations in surface hydrophobicity indicate that the hydrophilic groups of the HA molecule screen the hydrophobic groups; this prevents a quick attachment to hydrophobic surfaces.

#### Acknowledgments

The authors wish to thank H. P. van Leeuwen for his valuable comments and suggestions during the preparation of the manuscript. M.J.A. thanks the graduate school M&T and the Laboratory for Physical Chemistry & Colloid Science (Wageningen Agricultural University) for the first year postdoctoral fellowship and CONICET for the second one.

#### Literature Cited

- (1) Kinniburgh, D. G.; Milne, C. J.; Benedetti, M. F.; Pinheiro, J. P.; Filius, J.; Koopal, L. K.; van Riemsdijk, W. H. *Environ. Sci. Technol.* **1996**, *30*, 1687–1698.
- (2) Jones, M. N.; Bryan, N. *Adv. Colloid Interface Sci.* **1998**, *78*, 1–48.
- (3) McCarthy, J. F.; Zachara, J. M. *Environ. Sci. Technol.* **1989**, *23*, 496–502.
- (4) Murphy, E. M.; Zachara, J. M.; Smith, S. C. *Environ. Sci. Technol.* **1990**, *24*, 1507–1516.
- (5) Gu, B.; Schmitt, J.; Chen, Z.; Llang, L.; McCarthy, J. F. *Environ. Sci. Technol.* **1994**, *28*, 38–46.
- (6) Davis, J. A. In *Contaminants and Sediments*; Baker R. A., Ed.; Ann Arbor Sci.: Ann Arbor, 1981; Vol. 2, Chapter 15.
- (7) Vermeer, A. W. P.; Van Riemsdijk, W. H.; Koopal, L. K. *Langmuir* **1998**, *14*, 2810–2819.
- (8) Vermeer, A. W. P.; Koopal, L. K. *Langmuir* **1998**, *14*, 4210–4216.
- (9) Davis, J. A. *Geochim. Cosmochim. Acta* **1982**, *46*, 2381–2393.
- (10) Varadachari, C.; Chattopadhyay, T.; Ghosh, K. *Soil Sci.* **1997**, *162*, 28–34.
- (11) Gu, B.; Schmitt, J.; Chen, Z.; Llang, L.; McCarthy, J. F. *Geochim. Cosmochim. Acta* **1995**, *59*, 219–229.
- (12) Zhou, J. L.; Rowland, S. J.; Fauzi, R.; Mantoura, R. F. C.; Braven, J. *Water Res.* **1994**, *28*, 571–579.
- (13) Avena, M. J.; Koopal, L. K. *Environ. Sci. Technol.* **1998**, *32*, 2572–2577.
- (14) Pinheiro, J. P.; Mota, A. M.; Goncalves, M. S.; van Leeuwen, H. P. *Environ. Sci. Technol.* **1994**, *28*, 2112–2119.
- (15) Vermeer, A. W. P. Ph.D. Thesis, Agricultural University of Wageningen, 1996.
- (16) Avena, M. J.; Vermeer, A. W. P.; Koopal, L. K. *Colloids Surf.* **1999**, *151*, 213–224.
- (17) Beckett, R.; Hart, B. T. In *Environmental Particles*; Buffle, J., Van Leeuwen, H. P., Eds.; CRC Press: FL, 1993; pp 165–206.
- (18) Lyklema, J. *Fundamentals of Interface and Colloid Science*; Academic Press: London, 1995; Appendix 3, Vol. II.
- (19) Giatti, A.; Koopal, L. K. *J. Electroanal. Chem.* **1993**, *352*, 107–118.
- (20) Hoogeveen, N. G.; Cohen Stuart, M. A.; Fleer, G. J. *J. Colloid Interface Sci.* **1996**, *182*, 133–145.
- (21) Dijt, J. C.; Cohen Stuart, M. A.; Hofman, J. E.; Fleer, G. J. *Colloids Surf.* **1991**, *51*, 141–158.
- (22) Dijt, J. C. Ph.D. Thesis, Agricultural University of Wageningen, 1993.
- (23) Hansen, W. N. *J. Opt. Soc. Am.* **1968**, *58*, 380.
- (24) Ramsden, J. J. In *Biopolymers at Interfaces*; Surfactant Science Series 75; Malmsten, Ed.; Marcel Dekker: New York, 1998; Chapter 10.
- (25) Sauer, B. B.; Yu, H. *Macromolecules* **1989**, *22*, 786–791.
- (26) Cornell, P. K.; Summers, S. R.; Roberts, P. V. *J. Colloid Interface Sci.* **1986**, *110*, 149–164.
- (27) Pinheiro, J. P.; Mota, A. M.; Simoes Goncalves, M. L. S.; van Leeuwen, H. P. *Colloids Surf., A* **1998**, *137*, 165–170.
- (28) Pinheiro, J. P.; Mota, A. M.; Olivera J. M. R.; Martino, J. M. G. *Anal. Chim. Acta* **1996**, *329*, 15–24.
- (29) Engebretson, R. R.; von Wandruszka, R. *Environ. Sci. Technol.* **1994**, *28*, 1934–1941.
- (30) Reid, P. M.; Wilkinson, A. E.; Tippin, E.; Jones, M. N. *J. Soil Sci.* **1991**, *42*, 259–270.
- (31) Koopal, L. K.; Lee, E. M.; Böhmer, M. R. *J. Colloid Interface Sci.* **1995**, *170*, 85–97.
- (32) Koopal, L. K.; Goloub, T. In *Surfactant adsorption and surface solubilization*; Sharma, R., Ed.; ACS Symposium Series 165; American Chemical Society: Washington DC, 1995; pp 78–103.
- (33) Newcombe, G.; Drikas, M. *Carbon* **1997**, *35*, 1239–1250.

Received for review November 30, 1998. Revised manuscript received May 3, 1999. Accepted May 21, 1999.

ES981236U